Hydrol. Earth Syst. Sci. Discuss., https://doi.org/10.5194/hess-2018-638
Manuscript under review for journal Hydrol. Earth Syst. Sci.
Discussion started: 21 January 2019

Hydrology and Earth System Sciences
Discussions
Open Access

A global Budyko model to partition evaporation into interception and transpiration

Ameneh Mianabadi[1,2], Miriam Coenders–Gerrits[2*], Pooya Shirazi[1], Bijan Ghahraman[1], Amin Alizadeh[1]

1- Ferdowsi University of Mashhad, Mashhad, Iran
2- Delft University of Technology, Delft, The Netherlands

***Corresponding author**

Abstract

Evaporation is a very important flux in the hydrological cycle and links the water and energy balance of a catchment. The Budyko framework is often used to provide a first order estimate of evaporation, since it is a simple model where only rainfall and potential evaporation is required as input. Many researchers have tried to improve the Budyko framework by including more physics and catchment characteristics into the original equation. However, this often resulted in additional parameters, which are unknown or difficult to determine. In this paper we present an improvement of the previously presented Gerrits' model ("Analytical derivation of the Budyko curve based on rainfall characteristics and a simple evaporation model" in Gerrits et al, 2009 WRR), whereby total evaporation is calculated on the basis of simple interception and transpiration thresholds in combination with measurable parameters like rainfall dynamics and storage availability from remotely sensed data sources. While Gerrits' model was investigated for 10 catchments with different climate conditions and some parameters were assumed to be constant, in this study we applied the model on the global scale and fed with remotely sensed input data. The output of the model has been compared to two complex land-surface models STEAM and GLEAM, as well as the database of Landflux-EVAL. Our results show that total evaporation estimated by Gerrits' model is in good agreement with Landflux-EVAL, STEAM and GLEAM. Results also show that Gerrits' model underestimates interception in comparison to STEAM and overestimates it in comparison to GLEAM, while for transpiration the opposite is found. Errors in interception can partly be explained by differences in the interception definition that successively introduce errors in the calculation of transpiration. Comparing to the Budyko framework, the model showed a good performance for total evaporation estimation.

Keywords: Budyko curves, interception, transpiration, remote sensing, evaporation

Hydrol. Earth Syst. Sci. Discuss., https://doi.org/10.5194/hess-2018-638
Manuscript under review for journal Hydrol. Earth Syst. Sci.
Discussion started: 21 January 2019

Hydrology and Earth System Sciences
Open Access
Discussions

Introduction

Budyko curves are used as a first order estimate of annual evaporation as a function of annual precipitation and potential evaporation. If the available energy is sufficient to evaporate the available moisture, annual evaporation can approach annual precipitation (water-limited situation). If the available energy is not sufficient, annual evaporation can approach potential evaporation (energy-limited situation). Using the water balance and the energy balance and by applying the definition of the aridity index and Bowen ratio, the Budyko framework can be described as (Arora, 2002):

$$\frac{E_a}{P_a} = \frac{\emptyset}{1+f(\emptyset)} = F(\emptyset) \tag{1}$$

with E_a annual evaporation [L/T], P_a annual precipitation [L/T], $\frac{E_a}{P_a}$ the evaporation ratio [-], and $\emptyset$ the aridity index which is defined as the potential evaporation divided by annual precipitation [-]. Equation 1 is the base of all Budyko curves, which are developed by different researchers (Table 1).

The equations shown in Table 1 assume that the evaporation ratio is determined by climate only and do not take into account the effect of other controls on the water balance. Therefore, some researchers tried to incorporate more physics into the Budyko framework. For example Milly (1994, 1993) investigated the root zone storage as an important secondary control on the water balance. Choudhury (1999) used net radiation and a calibration factor in Budyko curves. Zhang et al. (2004, 2001) tried to add a plant-available water coefficient, Porporato et al. (2004) took into account the maximum storage capacity, Yang et al. (2006, 2008) incorporated a catchment parameter, and Donohue et al. (2007) tried to consider vegetation dynamics. Although the incorporation of these additional processes improved the model performance, the main difficulty with these approaches is the determination of the parameter values. In practice, they are therefore often used as calibration parameters. The model of Gerrits et al. (2009) (hereafter Gerrits' model) aimed to develop an analytical model that is physically based and only uses measurable parameters. They tested the model output (i.e., interception evaporation, transpiration, and total evaporation) on a couple of locations in the world, where the parameters could be determined, but not at the global scale due to data limitations. However, with the current developments in remotely sensed data new opportunities have arisen.

Recently, many studies (e.g., Chen et al., 2013; Donohue et al., 2010; Istanbulluoglu et al., 2012; Milly and Dunne, 2002; Wang, 2012; Zhang et al., 2008) found that soil moisture storage change is a critical component in modelling the interannual water balance. Including soil water information into the Budyko framework was often difficult, because this information is not widely available. However, Gao et al. (2014) presented a new method where the available soil water is derived from time series of rainfall and potential evaporation, plus a long-term runoff coefficient. This data can be derived locally (e.g., de Boer-Euser et al. (2016)), but can also be derived from remotely sensed data as shown by Wang-Erlandsson et al. (2016), which allows us to apply the method at the global scale and incorporate it in the Gerrits' model.

While Gerrits' model was only tested for 10 locations with different climatic conditions, the aim of this study is to test Gerrits' model at the global scale. We used remotely sensed data to estimate

Hydrol. Earth Syst. Sci. Discuss., https://doi.org/10.5194/hess-2018-638
Manuscript under review for journal Hydrol. Earth Syst. Sci.
Discussion started: 21 January 2019

parameters, which were considered constant in Gerrits' model. These parameters are the maximum soil moisture storage by the method of Gao et al (2014) and the interception storage capacity. These parameters are required to make a first order estimate of total evaporation, and to partition this into interception evaporation and transpiration as well. The outcome is compared to more complex land-surface-atmosphere models as well as to the Budyko curves of Table 1.

Methodology

Total evaporation (E) may be partitioned as follows (Shuttleworth, 1993):

$$E = E_i + E_t + E_o + E_s \tag{2}$$

in which E_i is interception evaporation, E_t is transpiration, E_o is evaporation from water bodies and E_s is evaporation from the soil, all with dimensions [LT^{-1}]. In this definition, interception is the amount of evaporation from any wet surface including canopy, understory, forest floor, and the top layer of the soil. Soil evaporation is defined as evaporation of the moisture in the soil that is connected to the root zone (de Groen and Savenije, 2006) and therefore is different from evaporation of the top layer of the soil (several millimeters of soil depth, which is here considered as part of the interception evaporation). Hence interception evaporation is the fast feedback of moisture to the atmosphere within a day from the rainfall event and soil evaporation is evaporation from the soil constrained by soil moisture storage in the root zone. Like Gerrits et al. (2009), we assume that evaporation from soil moisture is negligible (or can be combined with interception evaporation). Evaporation from water bodies is used for inland open water, where interception evaporation and transpiration is zero. As a result, Equation 2 becomes:

$$E = E_o \qquad \text{for water bodies} \tag{3a}$$
$$E = E_i + E_t \qquad \text{for land surface} \tag{3b}$$

where E_i is direct feedback from short term moisture storage on vegetation, ground, and top layer, and E_t is evaporation from soil moisture storage in the root zone.

For modelling evaporation, it is important to consider that interception and transpiration have different time scales (i.e. the stock divided by the evaporative flux) (Blyth and Harding, 2011). With a stock of a few millimetres and the evaporative flux of a few millimetres per day, interception has a time scale in the order of one day (Dolman and Gregory, 1992; Gerrits et al., 2009, 2007; Savenije, 2004; Scott et al., 1995). In the case of transpiration, the stock amounts to tens to hundreds of millimetres and the evaporative flux to a few millimetres per day (Baird and Wilby, 1999), resulting in a time scale in the order of month(s) (Gerrits et al., 2009). In Gerrits' model it is successively assumed that interception and transpiration can be modelled as threshold processes at the daily and monthly time scale, respectively. Rainfall characteristics are successively used to temporally upscale from daily to monthly, and from monthly to annual. A full description of the derivation and assumptions can be found in Gerrits et al. (2009). Here, we only summarize the relevant equations (Table 2) and not the complete derivation. Since we now test the model at the global scale, we do show how we estimated the required model parameters and the inputs used.

Hydrol. Earth Syst. Sci. Discuss., https://doi.org/10.5194/hess-2018-638
Manuscript under review for journal Hydrol. Earth Syst. Sci.
Discussion started: 21 January 2019

Interception

Gerrits' model considers evaporation from interception as a threshold process at daily time scale (Equation 4, Table 2). Daily interception ($E_{i,d}$), then, is upscaled to monthly interception ($E_{i,m}$, Equation 5, Table 2) by considering the frequency distribution of rainfall on a rain day (β-parameter) and subsequently to annual interception ($E_{i,a}$, Equation 6, Table 2) by considering the frequency distribution of rainfall in a rain month (κ_m-parameter) (see de Groen and Savenije (2006), Gerrits et al. (2009)). A rain day is defined as a day with more than 0.1 mm day^{-1} of rain and a rain month is a month with more than 2 mm month^{-1} of rain.

While Gerrits et al. (2009) assumed a constant interception threshold ($D_{i,d} = 5$ mm day^{-1}) for the studied locations, we here use a globally variable value based on remote sensing data. The interception threshold ($D_{i,d}$) is a yearly average and is either limited by the daily interception storage capacity S_{max} (mm day^{-1}) or by the daily potential evaporation (Equation 9, Table 2) and thus not seasonally variable. We can assume this, because for most locations S_{max} is smaller than $E_{p,d}$ even if we consider a daily varying potential evaporation. Additionally, S_{max} (based on LAI) could also be changed seasonally, however many studies show that the storage capacity is not changing significantly between the leafed and leafless period (e.g., Leyton et al., 1967; Dolman, 1987; Rutter et al., 1975). Especially, once interception is defined in a broad sense that it includes all evaporation from the canopy, understory, forest floor, and the top layer of the soil: leaves that are dropped from the canopy remain their interception capacity as they are on the forest floor in the leafless period. Furthermore, Gerrits et al (2010) showed with a Rutter-like model that interception is more influenced by the rainfall pattern than by the storage capacity, which was also found by Miralles et al. (2010). Hence, in interception modelling, the value of the storage capacity is of minor concern, and seasonality is incorporated in the temporal rainfall patterns.

The daily interception storage capacity should be seen as the maximum interception capacity within one day, including the (partly) emptying and filling of the storage between events per day, thus $S_{max} = n \cdot C_{max}$, where C_{max} [L] is the interception storage capacity of land cover. If there is only one rain event per day ($n = 1$ day^{-1}) (Gerrits et al., 2010), S_{max} [LT^{-1}] equals C_{max} [L], as is often found in literature. Despite proposing modifications for storms, which last more than one day (Pearce and Rowe, 1981), and multiple storms per rain day (Mulder, 1985), accounting for n is rarely necessary (Miralles et al., 2010).

For $n = 1$, the interception storage capacity can be estimated from Von Hoyningen-Huene (1981), which is obtained for a series of crops based on the leaf area index (LAI) (de Jong and Jetten, 2007) (Equation 10, Table 2). Since the storage capacity of the forest floor is not directly related to LAI, it could be said that the 0.935 mm in Equation 10 is sort of the storage capacity of the forest floor. Since this equation was developed for crops, it is likely that it underestimates interception by forests with a denser understory and forest floor interception capacity.

Transpiration

Hydrol. Earth Syst. Sci. Discuss., https://doi.org/10.5194/hess-2018-638
Manuscript under review for journal Hydrol. Earth Syst. Sci.
Discussion started: 21 January 2019

Transpiration is considered as a threshold process at the monthly time scale ($E_{t,m}$ (mm month^{-1}), Equation 7, Table 2) and successively is upscaled to annual transpiration ($E_{t,a}$ (mm year^{-1}), Equation 8, Table 2) by considering the frequency distribution of the net monthly rainfall ($P_{n,m} = P_m - E_{i,m}$) expressed with the parameter κ_n. To estimate the monthly and annual transpiration, two parameters A and B are required. A is the initial soil moisture or carryover value (mm month^{-1}) and B is dimensionless and described as Equation 15, where the dimensionless γ is obtained by Equation 16.

Gerrits et al. (2009) assumed that the carry over value (A) is constant and used $A = 0$, 5, 15, 20, mm month^{-1} , depending on the location, to determine annual transpiration. Also they considered γ to be constant ($\gamma = 0.5$). In the current study, we determined these two parameters based on the maximum root zone storage capacity ($S_{u,max}$). In equation 16, $\Delta t_m = 1$ month and S_b can be assumed to be 50% to 80% of $S_{u,max}$ (de Groen, 2002; Shuttleworth, 1993). In this study we assumed S_b to be 50% of $S_{u,max}$ as this value is commonly used for many crops (Allen et al., 1998). Furthermore, we assumed that the monthly carry over A can be estimated as $bS_{u,max}$ and in this study we assumed $b = 0.2$ which gave the best global results for all land classes. To estimate A and γ, it is important to have a reliable database of $S_{u,max}$. For this purpose, we used the global estimation of $S_{u,max}$ from Wang-Erlandsson et al. (2016) (Fig. 1d). $S_{u,max}$ is derived by the mass balance method using satellite based precipitation and evaporation (Wang-Erlandsson et al., 2016). Wang-Erlandsson et al. (2016) estimated the root zone storage capacity from the maximum soil moisture deficit, as the integral of the outgoing flux (i.e. evaporation which is sum of transpiration, evaporation, interception, soil moisture evaporation and open water evaporation) minus the incoming flux (i.e. precipitation and irrigation). In their study, the root zone storage capacity was defined as the total amount of water that plants can store to survive droughts. Note that this recent method (Gao et al., 2014) to estimate $S_{u,max}$ does not require soil information, but only uses climatic data. It is assumed that ecosystems adjust their storage capacity to climatic demands irrespective of the soil properties. Under wet conditions Gao's method appeared to perform better. For (semi-)arid climates the difference between this method and soil-based methods appear to be small (de Boer-Euser et al., 2016).

Furthermore, Gerrits et al. (2009) estimated the average monthly transpiration threshold ($D_{t,m}$) as $\frac{E_p - E_{i,a}}{n_a}$ (where n_a= number of months per year), which assumes that if there is little interception, plants can transpire at the same rate as a well-watered reference grass as calculated with the Penman-Monteith equation (University of East Anglia Climatic Research Unit , 2014). In reality, most plants encounter more resistance (crop resistance) than grass, hence we used Equation 17, Table 2 (Fredlund et al., 2012) to convert potential evaporation of reference grass (E_p) to potential transpiration of a certain crop depending on LAI (i.e. the transpiration threshold $D_{t,m}$ [mm month^{-1}]). Furthermore, similar to the daily interception threshold, we took a constant $D_{t,m}$, which can be problematic in energy-constrained areas. But in those relatively wet areas transpiration is underestimated in summer, but overestimated in winter, which will cancel out on the annual scale.

Data

For precipitation we used the AgMERRA product from AgMIP climate forcing dataset (Ruane et al., 2015), which has a daily time scale and a spatial resolution of 0.25°×0.25° (see Fig. 1a). The spatial coverage of AgMERRA is globally for the years 1980-2010. The AgMERRA product is available on the NASA Goddard Institute for Space Studies website (http://data.giss.nasa.gov/impacts/agmipcf/agmerra/).

Potential evaporation (see Fig. 1b) data (calculated by FAO-Penman–Monteith equation (Allen et al., 1998)) were taken from Center for Environmental Data Archival website (http://catalogue.ceda.ac.uk/uuid/4a6d071383976a5fb24b5b42e28cf28f), produced by the Climatic Research Unit (CRU) at the University of East Anglia (University of East Anglia Climatic Research Unit, 2014). These data are at the monthly time scale over the period 1901-2013, and has a spatial resolution of 0.5°×0.5°. We used the data of 1980-2010 in consistent with precipitation dataset.

LAI data (Fig. 1c) were obtained from Vegetation Remote Sensing & Climate Research (http://sites.bu.edu/cliveg/datacodes/) (Zhu et al., 2013). The spatial resolution of the data sets is 1/12 degree, with 15-day composites (2 per month) for the period July 1981 to December 2011.

The data of $S_{u,max}$ (Fig. 1d) is prepared data by Wang-Erlandsson et al. (2016) and is based on the satellite based precipitation and evaporation with 0.5°×0.5° resolution over the period 2003-2013. They used the USGS Climate Hazards Group InfraRed Precipitation with Stations (CHIRPS) precipitation data at 0.05° (Funk et al., 2014) and the ensemble mean of three datasets of evaporation including CSIRO MODIS Reflectance Scaling EvapoTranspiration (CMRSET) at 0.05° (Guerschman et al., 2009), the Operational Simplified Surface Energy Balance (SSEBop) at 30″ (Senay et al., 2013) and MODIS evapotranspiration (MOD16) at 0.05° (Mu et al., 2011). They calculated potential evaporation using Penman-Monteith equation (Monteith, 1965).

Model comparison and evaluation

The model performance was evaluated by comparing our results at the global scale to global evaporation estimates from other studies. Most available products only provide total evaporation estimates and do not distinguish between interception and transpiration. Therefore, we chose to compare our interception and transpiration results to two land surface models: The Global Land Evaporation Amsterdam Model (GLEAM) (v3.0a) database (Martens et al., 2017; Miralles et al., 2011a) and Simple Terrestrial Evaporation to Atmosphere Model (STEAM) (Wang-Erlandsson et al., 2014, Wang-Erlandsson et al., 2016). GLEAM estimates different fluxes of evaporation including transpiration, interception, bare soil evaporation, snow sublimation and open water evaporation. STEAM, on the other hand, estimates the different components of evaporation including transpiration, vegetation interception, floor interception, soil moisture evaporation, and open water evaporation. Thus for the comparison of interception we used the sum of canopy and floor interception and soil evaporation from STEAM and canopy interception and bare soil evaporation from GLEAM. Furthermore, STEAM includes an irrigation module (Wang-Erlandsson et al., 2014), while Miralles et al. (2011) mentioned that they did not include irrigation in GLEAM, but the assimilation of the soil moisture from satellite would account for it as soil moisture adjusted to seasonal dynamics of any region. The total evaporation was also compared to LandFlux-EVAL products (Mueller et al., 2013). GLEAM database (www.gleam.eu) is available for 1980-2014 with a resolution of 0.25°×0.25° and STEAM model was performed for 2003-2013 with a resolution of 1.5°×1.5°. LandFlux-EVAL data (https://data.iac.ethz.ch/landflux/) is available for 1989-2005. We compared Gerrits' model to other products based on the land cover to judge the performance of the model for different types of land cover. The global land cover map (Channan et al., 2014; Friedl et al., 2010) was obtained from http://glcf.umd.edu/data/lc/. Lastly, we also compared our results to the Budyko curves of Schreiber, O'ldekop, Pike and Budyko (Table 1). We used root mean square error (*RMSE*) (Eq. 20), mean bias error (*MBE*) (Eq. 21) and relative error (*RE*) (Eq. 22) to evaluate the results.

$$\mathrm{RMSE} = \sqrt{\frac{\sum_{i=1}^{n}(x_{iG} - x_{iM})^2}{n}} \tag{20}$$

$$\mathrm{MBE} = \frac{\sum_{i=1}^{n}(x_{iG} - x_{iM})}{n} \tag{21}$$

$$\mathrm{RE} = \frac{\bar{x}_G - \bar{x}_M}{\bar{x}_G} \times 100 \tag{22}$$

In these equations, x_{iM} is evaporation of the benchmark models to which Gerrits' model is compared for pixel i, x_{iG} is evaporation from Gerrits' model for pixel i, $\bar{x}_G$ is the average evaporation of Gerrits' model, $\bar{x}_M$ is the average evaporation of the benchmark models and n is the number of pixels of the evaporation map. Negative MBE and RE show the Gerrits' model underestimates evaporation and vice versa. As the spatial resolution of the products is different, we regridded all the products to the coarsest resolution (1.5°×1.5°) for the comparison. Furthermore, the comparisons were shown for each land cover using the Taylor diagram (Taylor, 2001). This diagram can provide a concise statistical summary of how the models are comparable to the reference data (observation or given model) in terms of their correlation, RMSE, and the ratio of their variances. In this paper, the reference data is Gerrits' model. Since the different models for different land cover types have been used in this study, which have different numerical values, the results are normalized by the reference data. It should be Noted that the standard deviation of the reference data is normalized by itself and, therefore, it is plotted at unit distance from the origin along the horizontal axis (Taylor, 2001). According to Taylor diagram, when the points are close to reference data (Ref in Figures 3, 5, 7 and 9), it shows that the RMSE is less and the correlation is higher and therefore, the models are in a more reasonable agreement.

Results and discussion

Total evaporation comparison

Figure 2 shows the mean annual evaporation from Gerrits' model, Landflux-EVAL, STEAM and GLEAM data sets. In general, the spatial distribution of Gerrits' simulated evaporation is similar to that of the benchmark models. Figure 2a demonstrates that, as expected, the highest annual evaporation, which is the sum of interception evaporation and transpiration, occurs in tropical evergreen broadleaf forests and the lowest rate occurs in the barren and sparsely vegetated desert regions. Total evaporation varies between almost zero in arid regions to more than 1500 mm year^{-1} in the tropics.

Hydrol. Earth Syst. Sci. Discuss., https://doi.org/10.5194/hess-2018-638
Manuscript under review for journal Hydrol. Earth Syst. Sci.
Discussion started: 21 January 2019

As can be seen in Figure 2 there exist also large differences between STEAM, GLEAM and Landflux-EVAL. Different products of precipitation (and other global data bases) applied for the models is likely the reason. For example, the sensitivity of the model to the number of rain days and rain months especially for the higher rate of precipitation (Gerrits et al., 2009) can be a probable reason for poor performance of a model especially for evergreen forests with the highest amount of precipitation.

Mean annual evaporation contributions per land cover type from Gerrits' model and other products as well as RMSE, MBE and RE are shown in Table 3. Globally, mean annual evaporation estimated (for the overlapped pixels with 1.5°×1.5° resolution) by Gerrits' model, Landflux-EVAL, STEAM and GLEAM are 443, 469, 475 and 462 mm year^{-1}, respectively. Our results are comparable to those of Haddeland et al. (2011), where the simulated global terrestrial evaporation ranges between 415 and 586 mm year^{-1} for the period 1985–1999. Generally, Gerrits' model overestimates evaporation for most land cover types in comparison to Landflux-EVAL and GLEAM, and underestimates in comparison to STEAM (see also MBE and RE). Since the number of pixels covered by each land use is different, RMSE, MBE and RE cannot be comparable between land cover types. RMSE, MBE and RE for each land cover type show that, generally, Gerrits' model is in a better agreement with Landflux and GLEAM than STEAM. The Taylor diagram for total evaporation estimated by Gerrits' model in comparison to Landflux-EVAL, STEAM and GLEAM for all data (No. 1 in Fig. 3) and for each land cover type (No.2 to No.11 in Fig. 3) also indicates that Gerrits' model has a better agreement with Landflux-EVAL and GLEAM than STEAM model, especially for Evergreen broadleaf forest, Shrublands, Savannas and Croplands (see also Table 3).

Annual interception comparison

While Wang-Erlandsson et al. (2014; 2016) estimated canopy interception, floor interception and soil evaporation separately, in the current study we assumed that these three components of evaporation can be lumped as interception evaporation. Figure 4 shows the mean annual evaporation from interception at the global scale estimated by Gerrits' model, STEAM and GLEAM. In this figure, interception from STEAM is calculated by the sum of canopy interception, floor interception and soil evaporation. Furthermore, interception from GLEAM is calculated as the sum of canopy interception and bare soil evaporation (GLEAM does not estimate floor interception). In general, the spatial distribution of Gerrits' simulated interception is partly similar to that of STEAM and GLEAM. In the tropics, with high amounts of annual precipitation and high storage capacity due to the dense vegetation (evergreen broadleaf forests and savannas), annual interception shows the highest values. Table 4 shows the average of interception, RMSE, MBE and RE per land cover type. This table indicates that Gerrits' model underestimates interception in comparison to STEAM for all land cover types. Table 4 also shows that, in comparison to GLEAM, Gerrits' model overestimates interception for all land cover types, because in GLEAM floor interception has not been taken into account. Figure 5 also shows that Gerrits' model is in better agreement with STEAM (especially for Grasslands and Mixed forest) than GLEAM. The reason for an underestimated interception in comparison to STEAM could be the role of the understory. LAI does not account for understory, therefore maybe S_{max} should be larger than modeled with Equation 10. However, there is almost no data available to estimate the interception storage capacity of the forest floor at the global scale.

We also compared our interception ratio E_i/E (Fig. 10) with some studies that looked after evaporation partitioning. Wang-Erlandsson defined interception in a slightly different way, hence we compared our calculated E_i/E with the sum of soil moisture evaporation ratio, vegetation interception ratio and floor interception ratio which are presented in Fig. 5.b, 5.c and 5.d in Wang-Erlandsson et al. (2014), respectively. While the results of Wang-Erlandsson et al. (2014) showed that vegetation interception in arid regions with no vegetation cover is zero, soil moisture and floor interception show a considerable percentage of total evaporation. Our results also show that $\frac{E_i}{E}$ in arid regions is close to 100%. Therefore, the interception ratio in this study is in a reasonable agreement with the results of Wang-Erlandsson et al. (2014). It is also comparable to the sum of bare soil evaporation and canopy interception from GLEAM (Martens et al., 2017).

Annual transpiration comparison

Figure 6 illustrates the mean annual transpiration estimated by Gerrits' model, STEAM and GLEAM. The spatial distribution is similar to the results of STEAM and GLEAM. Mean annual transpiration varies between zero mm year^{-1} for arid areas in the north of Africa (Sahara) to more than 1000 mm year^{-1} in the tropics in South America. The results show that the highest annual transpiration occurrs in Evergreen broadleaf forests with the highest amount of precipitation and dense vegetation (see also Table 5). Figure 6c shows that GLEAM, in comparison to Gerrits' model, overestimates the transpiration in some regions especially in the tropics in South America and Central Africa. Figure 6b also shows that STEAM is different from Gerrits' model over some regions like India, western China and North America as well as in the tropics. Table 5 (MBE and RE) also indicates that Gerrits' model underestimates transpiration in comparison to GLEAM and overestimates in comparison to STEAM. The Taylor diagram (Fig. 7) shows global annual transpiration of Gerrits' model is closer to that of GLEAM than STEAM, representing that the Gerrits' model is in a more reasonable agreement with GLEAM for transpiration estimation.

Similar to the interception ratio, we also compared our transpiration ratio E_t/E (Fig 10), and found that the results are in a reasonable agreement with STEAM (See Fig. 5.a, Wang-Erlandsson et al. (2014)) and GLEAM (See Fig. 9.e, Martens et al. (2017)). Global transpiration ratio estimated by Gerrits' model is 71% which is comparable to the ratio estimated by other studies (e.g. 80% (Miralles et al., 2011b), 69% (Sutanto, 2015),65% (Good et al., 2015), 62% (Maxwell and Condon, 2016), 62% (Lian et al., 2018), 61% (Schlesinger and Jasechko, 2014) 60% (Coenders-Gerrits et al., 2014), 57% (Wei et al., 2017)), 52% (Choudhury and Digirolamo, 1998), 48% (Dirmeyer et al., 2006) and 41% (Lawrence et al., 2007). The spatial pattern of transpiration ratio is a reasonable agreement with those of Wei et al. (2017) and Schlesinger and Jasechko (2014).

Budyko framework

Figure 8 shows the mean annual evaporation derived from four non-parametric Budyko curves (Table 1) including Schreiber (1904), Ol'dekop (1911), Pike (1964) and Budyko (1974). The global mean annual evaporation estimated by Pike and Budyko are close (445 and 439 mm year^{-1}, respectively). Schreiber underestimates the mean annual evaporation in comparison to Ol'dekop, Pike and Budyko, especially in regions with a higher rate of evaporation. Table 6 shows the mean annual evaporation estimated by these four curves per land cover type in comparison to Gerrits' model as well as RMSE, MBE and RE. The results show that mean annual evaporation of Gerrits'

Hydrol. Earth Syst. Sci. Discuss., https://doi.org/10.5194/hess-2018-638
Manuscript under review for journal Hydrol. Earth Syst. Sci.
Discussion started: 21 January 2019

model for forests is closer to that of Ol'dekop and for the other land classes it is closer to that of Budyko. Global mean annual evaporation is close to Pike where RE is almost zero. Taylor diagram (Fig. 9) shows that, in comparison to the Budyko curves, Gerrits' model performs well for all land cover types except for Evergreen broadleaf and Deciduous needleleaf forest. Evergreen broadleaf forest shows a significant overestimation of evaporation by Gerrits' model in comparison to Budyko curves. One of the reasons for these differences can be the used precipitation product as Gerrits et al. (2009) mentioned that the number of rain months per year, is the most sensitive parameter. Furthermore, as mentioned before in Section "Annual interception comparison", the role of the understory, which has not been taken into account in S_{max} equation, can be a source of error for the poor interception performance (and therefore total evaporation) in forests.

Conclusion

In the current study we improved and applied a simple evaporation model proposed by Gerrits et al. (2009) at the global scale. Instead of locally calibrated model parameters we now only used parameters derived from remotely sensed data. Furthermore, we implemented in the Gerrits' model a new definition of the root zone storage capacity from Gao et al (2014).

Comparing our results for total evaporation to Landflux-EVAL estimates show that Gerrits' model is in good agreement with Landflux-EVAL. The highest mean annual evaporation rates are found in evergreen broadleaf forests (1367 mm year^{-1}), deciduous broadleaf forests (796 mm year^{-1}) and savannas (695 mm year^{-1}) and the lowest ones are found in shrublands (203 mm year^{-1}) and grasslands (275 mm year^{-1}). Generally, Gerrits' model overestimates in comparison to Landflux-EVAL and GLEAM, and underestimates in comparison to STEAM.

Gerrits' model underestimates interception in comparison to STEAM for all land covers. On the other hand, the model overestimates interception in comparison to GLEAM, since GLEAM does not include floor interception. Although we tried to correct for the different definitions of interception, the results may be biased. The relatively worse performance in forests ecosystems could be explained by the effect of understory. This is not taken into account in Gerrits' model, while the understory can also intercept water. We could say that the constant value of 0.935 mm in Equation 10 reflects the forest floor interception storage capacity, but since this number was derived for crops, it is likely an underestimation. Therefore, better estimation of S_{max} to account for forest floor interception is recommended.

Estimated transpiration by Gerrits' model is in reasonable agreement with GLEAM and STEAM. Gerrits' model underestimates transpiration in comparison to GLEAM (RE=-4%) and overestimates in comparison to STEAM (RE=+12%). The scatter plots showed that, in comparison to GLEAM and STEAM, Gerrits' model performs well for all land cover types. Also the transpiration ratio corresponded well in comparison to those of GLEAM and STEAM. The results also showed that the global transpiration ratio estimated by Gerrits' model (71%) is approximately comparable to the other studies.

Comparing Gerrits' model to some Budyko curves, shows that the model performed well, but in areas with few number of rain months, evaporation is not close to the Budyko curves of Schreiber, Ol'dekop, Pike and Budyko. This is likely caused by the fact that Gerrits' model is rather sensitive to the number of rain days and rain months.

Comparing all products, we found that, in general, there are large differences between STEAM, GLEAM and Landflux-EVAL. The most convincing reason for this discrepancy lies in the different products for precipitation (and different global data sets), which have been used for the different models. The Gerrits' model is sensitive to the number of rain days and months especially for the higher rates of precipitation. Therefore, for evergreen forest with the highest amount of precipitation, this can be a probable reason for discrepancies.

Generally, it should be mentioned that the underlying reasoning of the Gerrits' model is to recognize the characteristic time scales of the different evaporation processes (i.e. interception daily and transpiration monthly). In Gerrits et al. (2009) (and in the current paper as well), this has been done by taking yearly averages for the interception ($D_{i,d}$, mm day^{-1}) and transpiration threshold ($D_{t,m}$, mm month^{-1}) in combination with the temporal distribution functions for daily and monthly (net) rainfall. Hence, the seasonality is incorporated in the temporal rainfall patterns, and not in the evaporation thresholds. This is a limitation of the currently used approach and could be the focus of a new study by investigating how seasonal fluctuating thresholds (based on LAI and/or a simple cosine function) would affect the results. This could be a significant methodological improvement of the Gerrits' model, but will have mathematical implications on the analytical model derivation. It will improve the monthly evaporation estimates, but we expect that the consequences at the annual time scale (which is the focus of the current paper) will be less severe. The strength of the Gerrits' model is that, in comparison to other models, it is a very simple and in spite of its simplicity, the Gerrits' model performs quite well.

Acknowledgment

This research was partly funded by NWO Earth and Life Sciences (ALW), veni-project 863.15.022, the Netherlands. Furthermore, we would like to thank Iran's Ministry of Science, Research and Technology for supporting this research and the mobility fellowship. We also would like to thank Jie Zhou, Lan Wang-Erlandsson, Kamran Davary, Shervan Gharari and Hubert Savenije for their kind helps and comments.

References

Allen, R., Pereira, L., Raes, D., Smith, M.: Crop evapotranspiration: Guidelines for computing crop water requirements. FAO Irrig. Drain. Pap. 56. FAO, Rome, Italy, 300 p, 1998.

Arora, V.K.: The use of the aridity index to assess climate change effect on annual runoff. J. Hydrol. 265, 164–177, doi:10.1016/S0022-1694(02)00101-4, 2002.

Baird, A.J., Wilby, R.L.: Eco-hydrology: Plants and Water in Terrestrial and Aquatic Environments. Routledge, London, 1999.

Blyth, E., Harding, R.J.: Methods to separate observed global evapotranspiration into the interception , transpiration and soil surface evaporation components. Hydrol. Process. 25, 4063–4068, doi:10.1002/hyp.8409, 2011.

Budyko, M.I.: Climate and life. Academic Press, Orlando, Fla, 1974.

Channan, S., Collins, K., Emanuel, W.R.: Global mosaics of the standard MODIS land cover type data. College Park, Maryland, USA, 2014.

Chen, X., Alimohammadi, N., Wang, D.: Modeling interannual variability of seasonal evaporation and storage change based on the extended Budyko framework. Water Resour. Res. 49, 6067–6078, doi:10.1002/wrcr.20493, 2013.

Choudhury, B.: Evaluation of an empirical equation for annual evaporation using field observations and results from a biophysical model. J. Hydrol. 216, 99–110, doi:10.1016/S0022-1694(98)00293-5, 1999.

Choudhury, B., Digirolamo, N.E.: A biophysical process-based estimate of global land surface evaporation using satellite and ancillary data I . Model description and comparison with observations. J. Hydrol. 205, 164–185, 1998.

Coenders-Gerrits, A.M.J., van der Ent, R.J., Bogaard, T.A., Wang-Erlandson, L., Hrachowitz, M., Savenije, H.H.G.: Uncertainties in transpiration estimates. Nature 506, E1–E2, doi:10.1038/nature12925, 2014.

de Boer-Euser, T., McMillan, H.K., Hrachowitz, M., Winsemius, H.C., Savenije, H.H.G.: Influence of soil and climate on root zone storage capacity. Water Resour. Res. 17, doi:10.1002/2015WR018115, 2016.

de Groen, M.M.: Modelling interception and transpiration at monthly time steps : introducing daily variability through Markov chains, 2002.

de Groen, M.M., Savenije, H.H.G.: A monthly interception equation based on the statistical characteristics of daily rainfall. Water Resour. Res. 42, W12417, doi:10.1029/2006WR005013, 2006.

de Jong, S.M., Jetten, V.G.: Estimating spatial patterns of rainfall interception from remotely sensed vegetation indices and spectral mixture analysis. Int. J. Geogr. Inf. Sci. 21, 529–545, doi:10.1080/13658810601064884, 2007.

Dirmeyer, P.A., Gao, X., Zha, M., Guo, Z., Oki, T., Hanasaki, N.: GSWP-2: Multimodel analysis and implications for our per- ception of the land surface. Bull. Am. Meteorol. Soc. 87, 1381–1397, doi:10.1175/BAMS-87-10-1381, 2006.

Dolman, a J., Gregory, D.: The Parametrization of Rainfall Interception In GCMs. Q. J. R. Meteorol. Soc. 118, 455–467, doi:10.1002/qj.49712051713, 1992.

Donohue, R.J., Roderick, M.L., Mcvicar, T.R.: On the importance of including vegetation dynamics in Budyko ' s hydrological model. Hydrol. Earth Syst. Sci. 11, 983–995, 2007.

Donohue, R.J., Roderick, M.L., McVicar, T.R.: Can dynamic vegetation information improve the accuracy of Budyko's hydrological model? J. Hydrol. 390, 23–34, doi:10.1016/j.jhydrol.2010.06.025, 2010.

Fredlund, D.G., Rahardjo, H., Fredlund, M.D.: Unsaturated Soil Mechanics in Engineering Practice. John Wiley & Sons, Ltd., doi:10.1002/9781118280492, 2012.

Friedl, M.A., Sulla-Menashe, D., Tan, B., Schneider, A., Ramankutty, N., Sibley, A., Huang, X.: MODIS Collection 5 global land cover: Algorithm refinements and characterization of new datasets, 2001-2012, Collection 5.1 IGBP Land Cover. Boston, MA, USA, 2010.

Gao, H., Hrachowitz, M., Schymanski, S.J., Fenicia, F., Sriwongsitanon, N., Savenije, H.H.G.: Climate controls how ecosystems size the root zone storage capacity at catchment scale. Geophys. Res. Lett. 41, 7916–7923, doi:10.1002/2014GL061668, 2014.

Gerrits, A.M.J., Pfister, L., Savenije, H.H.G.: Spatial and temporal variability of canopy and forest floor interception in a beech forest. Hydrol. Process. 24, 3011–3025, doi:10.1002/hyp.7712, 2010.

Gerrits, A.M.J., Savenije, H.H.G., Hoffmann, L., Pfister, L.: New technique to measure forest floor interception – an application in a beech forest in Luxembourg. Hydrol. Earth Syst. Sci. 11, 695–701, doi:10.5194/hess-11-695-2007, 2007.

Gerrits, A.M.J., Savenije, H.H.G., Veling, E.J.M., Pfister, L.: Analytical derivation of the Budyko curve based on rainfall characteristics and a simple evaporation model. Water Resour. Res. 45, W04403, doi:10.1029/2008WR007308, 2009.

Good, S.P., Noone, D., Bowen, G.: Hydrologic connectivity constrains partitioning of global terrestrial water fluxes. Science (80), 349, 175–177, 2015.

Guerschman, J.P., Van Dijk, A.I.J.M., Mattersdorf, G., Beringer, J., Hutley, L.B., Leuning, R., Pipunic, R.C., Sherman, B.S.: Scaling of potential evapotranspiration with MODIS data reproduces flux observations and catchment water balance observations across Australia. J. Hydrol. 369, 107–119, doi:10.1016/j.jhydrol.2009.02.013, 2009.

Haddeland, I., Clark, D.B., Franssen, W., Ludwig, F., Voß, F., Arnell, N.W., Bertrand, N., Best, M., Folwell, S., Gerten, D., Gomes, S., Gosling, S.N., Hagemann, S., Hanasaki, N., Harding, R., Heinke, J., Kabat, P., Koirala, S., Oki, T., Polcher, J., Stacke, T., Viterbo, P., Weedon, G.P., Yeh, P.: Multimodel Estimate of the Global Terrestrial Water Balance : Setup and First Results. J. Hydrometeorol. 12, 869–884, doi:10.1175/2011JHM1324.1, 2011.

Istanbulluoglu, E., Wang, T., Wright, O.M., Lenters, J.D.: Interpretation of hydrologic trends from a water balance perspective: The role of groundwater storage in the Budyko hypothesis. Water Resour. Res. 48, W00H16, doi:10.1029/2010WR010100, 2012.

Lawrence, D.M., Thornton, P.E., Oleson, K.W., Bonan, G.B.: The Partitioning of Evapotranspiration into Transpiration , Soil Evaporation , and Canopy Evaporation in a GCM : Impacts on Land – Atmosphere Interaction. J. Hydrometeorol. 8, 862–880, doi:10.1175/JHM596.1, 2007.

Lian, X., Piao, S., Huntingford, C., Li, Y., Zeng, Z., Wang, X., Ciais, P., Mcvicar, T.R., Peng, S., Ottlé, C., Yang, H., Yang, Y., Zhang, Y., Wang, T.: CMIP5 models constrained by observations. Nat. Clim. Chang. 8, 640–646, doi:10.1038/s41558-018-0207-9, 2018.

Martens, B., Miralles, D.G., Lievens, H., Van Der Schalie, R., De Jeu, R.A.M., Fernández-Prieto, D., Beck, H.E., Dorigo, W.A., Verhoest, N.E.C.: GLEAM v3 : satellite-based land evaporation and root-zone soil moisture. Geosci. Model Dev. 10, 1903–1925, doi:10.5194/gmd-10-1903-2017, 2017.

Maxwell, R.M., Condon, L.E.: Connections between groundwater flowand transpiration partitioning. Science (80). 353, 377–380, 2016.

Milly, P.C.D.: Climate, soil water storage, and the average annual water balance. Water Resour. Res. 30, 2143–2156, doi:10.1029/94WR00586, 1994.

Milly, P.C.D.: An analytic solution of the stochastic storage problem applicable to soil water. Water Resour. Res. 29, 3755–3758, doi:10.1029/93WR01934, 1993.

Milly, P.C.D., Dunne, K. A.: Macroscale water fluxes 2. Water and energy supply control of their interannual variability. Water Resour. Res. 38, 24-1-24–9, doi:10.1029/2001WR000760, 2002.

Miralles, D.G., De Jeu, R.A.M., Gash, J.H., Holmes, T.R.H., Dolman, A.J.: Magnitude and variability of land evaporation and its components at the global scale. Hydrol. Earth Syst. Sci. 15, 967–981, doi:10.5194/hess-15-967-2011, 2011.

Miralles, D.G., Gash, J.H., Holmes, T.R.H., De Jeu, R.A.M., Dolman, A.J.: Global canopy interception from satellite observations. J. Geophys. Res. Atmos. 115, 1–8, doi:10.1029/2009JD013530, 2010.

Miralles, D.G., Holmes, T.R.H., De Jeu, R.A.M., Gash, J.H., Meesters, A.G.C.A., Dolman, A.J.: Global land-surface evaporation estimated from satellite-based observations. Hydrol. Earth Syst. Sci. 15, 453–469, doi:10.5194/hess-15-453-2011, 2011.

Mu, Q., Zhao, M., Running, S.W.: Improvements to a MODIS global terrestrial evapotranspiration algorithm. Remote Sens. Environ. 115, 1781–1800, doi:10.1016/j.rse.2011.02.019, 2011.

Mueller, B., Hirschi, M., Jimenez, C., Ciais, P., Dirmeyer, P.A., Dolman, A.J., Fisher, J.B., Jung, M., Ludwig, F., Maignan, F., Miralles, D.G., McCabe, M.F., Reichstein, M., Sheffield, J., Wang, K., Wood, E.F., Zhang, Y., Seneviratne, S.I.: Benchmark products for land evapotranspiration: LandFlux-EVAL multi-data set synthesis. Hydrol. Earth Syst. Sci. 17, 3707–3720, doi:10.5194/hess-17-3707-2013, 2013.

Mulder, J.P.M.: Simulating Interception Loss Using Standard Meteorological Data, in: Hutchison, B.A., Hicks, B.B. (Eds.), The Forest-Atmosphere Interaction. pp. 177–196, 1985.

Ol'dekop, E.M.: On evaporation from the surface of river basins. Trans. Meteorol. Obs. 4, 200, 1911.

Pearce, A.J., Rowe, L.K.: Rainfall interception in a multi-storied, evergreen mixed forest: estimates using {G}ash's analytical model. J. Hydrol. 49, 341–353, doi:10.1016/S0022-1694(81)80018-2, 1981.

Pike, J.G.: The estimation of annual run-off from meteorological data in a tropical climate. J. Hydrol. 2, 116–123, doi:10.1016/0022-1694(64)90022-8, 1964.

Porporato, A., Daly, E., Rodriguez-Iturbe, I.: Soil water balance and ecosystem response to climate change. Am. Nat. 164, 625–632, doi:10.1086/521238, 2004.

Ruane, A.C., Goldberg, R., Chryssanthacopoulos, J.: Climate forcing datasets for agricultural modeling: Merged products for gap-filling and historical climate series estimation. Agric. For. Meteorol. 200, 233–248, doi:10.1016/j.agrformet.2014.09.016, 2015.

Savenije, H.H.G.: The importance of interception and why we should delete the term evapotranspiration from our vocabulary. Hydrol. Process. 18, 1507–1511, doi:10.1002/hyp.5563, 2004.

Schlesinger, W.H., Jasechko, S.: Transpiration in the global water cycle. Agric. For. Meteorol.

Hydrology and Earth System Sciences
Open Access
Discussions

189–190, 115–117, doi:10.1016/j.agrformet.2014.01.011, 2014.

Schreiber, P.: About the relationship between the precipitation and the water management of the river in Central Europe. Meteorology 21, 441– 452, 1904.

Scott, R., Koster, R.D., Entekhabi, D., Suarez, M.J.: Effect of a Canopy Interception Reservoir on Hydrological Persistence in a General Circulation Model. J. Clim. 8, 1917–1922, doi:10.1175/1520-0442(1995)008<1917:EOACIR>2.0.CO;2, 1995.

Senay, G.B., Bohms, S., Singh, R.K., Gowda, P.H., Velpuri, N.M., Alemu, H., Verdin, J.P.: Operational Evapotranspiration Mapping Using Remote Sensing and Weather Datasets: A New Parameterization for the SSEB Approach. J. Am. Water Resour. Assoc. 49, 577–591, doi:10.1111/jawr.12057, 2013.

Shuttleworth, W.J.: Evaporation, in: Handbook of Hydrology. McGraw-Hill, New York, p. 4.1-4.53, 1993.

Sutanto, S.J.: Global transpiration fraction derived from water isotopologue datasets. J. Tek. Hidraul. 6, 131–146, 2015.

Taylor, K.E.: Summarizing multiple aspects of model performance in a single diagram. J. Geophys. Res. 106, 7183–7192, 2001.

University of East Anglia Climatic Research Unit, Harris, I.C., Jones, P.D.: CRU TS3.22: Climatic Research Unit (CRU) Time-Series (TS) Version 3.22 of High Resolution Gridded Data of Month-by-month Variation in Climate (Jan. 1901- Dec. 2013). NCAS Br. Atmos. Data Cent. 24 Septemb, doi:10.5285/18BE23F8-D252-482D-8AF9-5D6A2D40990C, 2014.

Von Hoyningen-Huene, J.: Die Interzeption des Niederschlags in Landwirtschaftlichen Pflanzenbesta¨nden. Arbeitsbericht Dtsch. Verband fur Wasserwirtschaft und Kult. (Braunschweig DVWK), 1981.

Wang-erlandsson, L., Bastiaanssen, W.G.M., Gao, H., Jägermeyr, J., Senay, G.B., Dijk, A.I.J.M. Van, Guerschman, J.P., Keys, P.W., Gordon, L.J., Savenije, H.H.G.: Global root zone storage capacity from satellite-based evaporation. Hydrol. Earth Syst. Sci. 20, 1459–1481, doi:10.5194/hess-20-1459-2016, 2016.

Wang-Erlandsson, L., Bastiaanssen, W.G.M., Gao, H., Jägermeyr, J., Senay, G.B., van Dijk, A.I.J.M., Guerschman, J.P., Keys, P.W., Gordon, L.J., Savenije, H.H.G.: Global root zone storage capacity from satellite-based evaporation. Hydrol. Earth Syst. Sci. Discuss. 1–49, doi:10.5194/hess-2015-533, 2016.

Wang-Erlandsson, L., Van Der Ent, R.J., Gordon, L.J., Savenije, H.H.G.: Contrasting roles of interception and transpiration in the hydrological cycle - Part 1: Temporal characteristics over land. Earth Syst. Dyn. 5, 441–469, doi:10.5194/esd-5-441-2014, 2014.

Wang, D.: Evaluating interannual water storage changes at watersheds in Illinois based on long-term soil moisture and groundwater level data. Water Resour. Res. 48, doi:10.1029/2011WR010759, 2012.

Wei, Z., Yoshimura, K., Wang, L., Miralles, D., Jasechko, S., Lee, X.: Revisiting the contribution of transpiration to global terrestrial evapotranspiration. Am. Geophys. Union, doi:10.1002/2016GL072235, 2017.

Yang, D., Sun, F., Liu, Z., Cong, Z., Lei, Z.: Interpreting the complementary relationship in nonhumid environments based on the Budyko and Penman hypotheses. Geophys. Res. Lett. 33, 1–5, doi:10.1029/2006GL027657, 2006.

Yang, H., Yang, D., Lei, Z., Sun, F.: New analytical derivation of the mean annual water-energy balance equation. Water Resour. Res. 44, W03410, doi:10.1029/2007WR006135, 2008.

Zhang, L., Dawes, W.R., Walker, G.R.: Response of Mean Annual Evapotranspiration to Vegetationchanges at Catchment Scale. Water Resour. 37, 701–708, 2001.

Zhang, L., Hickel, K., Dawes, W.R., Chiew, F.H.S., Western, A.W., Briggs, P.R.: A rational function approach for estimating mean annual evapotranspiration. Water Resour. Res. 40, WR002710, doi:10.1029/2003WR002710, 2004.

Zhang, L., Potter, N., Hickel, K., Zhang, Y., Shao, Q., Water balance modeling over variable time scales based on the Budyko framework – Model development and testing. J. Hydrol. 360, 117–131, doi:10.1016/j.jhydrol.2008.07.021, 2008.

Zhu, Z., Bi, J., Pan, Y., Ganguly, S., Anav, A., Xu, L., Samanta, A., Piao, S., Nemani, R.R., Myneni, R.B.: Global data sets of vegetation leaf area index (LAI)3g and fraction of photosynthetically active radiation (FPAR)3g derived from global inventory modeling and mapping studies (GIMMS) normalized difference vegetation index (NDVI3G) for the period 1981 to 2. Remote Sens. 5, 927–948, doi:10.3390/rs5020927, 2013.

Hydrol. Earth Syst. Sci. Discuss., https://doi.org/10.5194/hess-2018-638
Manuscript under review for journal Hydrol. Earth Syst. Sci.
Discussion started: 21 January 2019

Table 1- Budyko equations developed by different researchers.

Equation	Reference
$\frac{E_a}{P_a} = 1 - \exp(-\emptyset)$	Schreiber [1904]
$\frac{E_a}{P_a} = \emptyset\tanh(\frac{1}{\emptyset})$	Ol'dekop [1911]
$\frac{E_a}{P_a} = \frac{1}{\sqrt{0.9 + (\frac{1}{\emptyset})^2}}$	Turc [1954]
$\frac{E_a}{P_a} = \frac{1}{\sqrt{1 + (\frac{1}{\emptyset})^2}}$	Pike [1964]
$\frac{E_a}{P_a} = [\emptyset \tanh\left(\frac{1}{\emptyset}\right)(1 - \exp(-\emptyset))]^{1/2}$	Budyko [1974]

Table 2- Summary of the interception and transpiration equations of Gerrits' model (Gerrits et al., 2009)

Equation	Equation number	Description
$E_{i,d} = \min(D_{i,d}, P_d)$	(4)	$E_{i,d}$: daily interception (mm day^{-1}), P_d: daily precipitation (mm day^{-1}), $D_{i,d}$: the daily interception threshold (mm day^{-1})
$E_{i,m} = P_m\left(1 - \exp(-\emptyset_{i,m})\right)$	(5)	$E_{i,m}$: monthly interception (mm month^{-1}), P_m: monthly rainfall (mm month^{-1}), $\emptyset_{i,m}$: a sort of aridity index for interception at monthly scale
$E_{i,a} = P_a(1 - 2\emptyset_{ia}K_0(2\sqrt{\emptyset_{i,a}}) - 2\sqrt{\emptyset_{i,a}}K_1(2\sqrt{\emptyset_{i,a}}))$	(6)	$E_{i,a}$: annual interception (mm year^{-1}), P_a: annual rainfall (mm year^{-1}), $\emptyset_{i,a}$: a sort of aridity index for interception at annual scale, K_0 and K_1: the Bessel function of the first and second order, respectively
$E_{t,m} = \min(A + B(P_m - E_{i,m}), D_{t,m})$	(7)	$E_{t,m}$: monthly transpiration (mm month^{-1}), A: carry-over parameter (mm month^{-1}), $D_{t,m}$: the transpiration threshold (mm month^{-1}), B: slope of relation between monthly effective rainfall and monthly transpiration
$E_{t,a} = 2BP_a\left(\emptyset_{i,a}K_0(2\sqrt{\emptyset_{i,a}}) + \sqrt{\emptyset_{i,a}}K_1(2\sqrt{\emptyset_{i,a}})\right)$ $\left(\frac{A}{\kappa_n B} + 1 - \exp(-\emptyset_{t,a})\left(\frac{A}{\kappa_n B} + 1 + \emptyset_{t,a} - \frac{\emptyset_{t,a}}{B}\right)\right)$	(8)	$E_{t,a}$: annual transpiration (mm year^{-1}), $\emptyset_{t,a}$: an aridity index
$D_{i,d} = \min(S_{max}, E_{p,d})$	(9)	S_{max}: the daily interception storage capacity (mm day^{-1}) $E_{p,d}$: the daily potential evaporation, $E_{p,a}$: annual potential evaporation (mm year^{-1})
$S_{max} \approx C_{max} = 0.935 + 0.498\mathrm{LAI} - 0.00575\mathrm{LAI}^2$	(10)	LAI: Leaf Area Index derived from remote sensing images
$\emptyset_{i,m} = \frac{D_{i,d}}{\beta}$	(11)	β: scaling factor
$\beta = \frac{P_m}{E(n_{r,d}\|n_m)}$	(12)	$E(n_{r,d}\|n_m)$: the expected number of rain days per month, $n_{r,d}$: the number of rain days per month, n_m: the number of days per month
$\emptyset_{i,a} = \frac{n_{r,d}D_{i,d}}{\kappa_m}$	(13)	κ_m: scaling factor for monthly rainfall
$\kappa_m = \frac{P_a}{E(n_{r,m}\|n_a)}$	(14)	$E(n_{r,m}\|n_a)$: the expected number of rain months per year, $n_{r,m}$: the number of rain months per year, n_a: the number of months per year
$B = 1 - \gamma + \gamma\exp(-\frac{1}{\gamma})$	(15)	γ: time scale for transpiration
$\gamma = \frac{S_b}{D_{t,m}\Delta t_m}$	(16)	S_b: the moisture content below which transpiration is restricted (mm).
$D_{t,m} = 0 \quad for\ LAI < 0.1$ $D_{t,m} = \frac{E_p}{n_a}(-0.21 + 0.7LAI^{0.5}) \quad for\ 0.1 \le LAI < 2.7$ $D_{t,m} = \frac{E_p}{n_a} \quad for\ LAI \ge 2.7$	(17)	E_p: annual potential evaporation (for open water) (mm year^{-1})
$\emptyset_{t,a} = \frac{D_{t,m}}{\kappa_n}$	(18)	κ_n: scaling factor for monthly net rainfall
$\kappa_n = \frac{P_{n,a}}{E(n_{nr,m}\|n_a)} = \frac{P_a - E_{i,a}}{E(n_{nr,m}\|n_a)}$	(19)	$P_{n,a}$: annual net precipitation, $E(n_{nr,m}\|n_a)$: the expected number of net rain months per year

Hydrol. Earth Syst. Sci. Discuss., https://doi.org/10.5194/hess-2018-638
Manuscript under review for journal Hydrol. Earth Syst. Sci.
Discussion started: 21 January 2019

Table 3- Comparison of mean annual evaporation estimated by Gerrits' model to Landflux-EVAL, STEAM and GLEAM through Average, RMSE, MBE and RE per land cover type. Negative MBE and RE show the Gerrits' model underestimates evaporation and vice versa. Average, RMSE and MBE are in mm $year^{-1}$ and RE is in %.

Land cover	area	Gerrits	Landflux-EVAL				STEAM				GLEAM			
	$1000km^2$	Avg.*	Avg.	RMSE	MBE	RE	Avg.	RMSE	MBE	RE	Avg.	RMSE	MBE	RE
Evergreen needleleaf forest	5563	430	387	122	+43	+10	467	150	-37	-9	457	127	-27	-6
Evergreen broadleaf forest	11778	1367	1177	266	+190	+14	1129	345	+238	+17	1244	225	+123	+9
Deciduous needleleaf forest	2498	338	298	73	+40	+12	336	65	+2	+1	336	73	+1	0
Deciduous broadleaf forest	1106	796	736	138	+61	+8	840	215	-44	-6	660	197	+136	+17
Mixed forest	13470	563	487	136	+76	+13	545	137	+18	+3	527	131	+35	+6
Shrublands[1]	29542	203	259	96	-57	-28	262	123	-59	-29	253	91	-51	-25
Savannas[2]	18846	695	739	148	-44	-6	737	186	-42	-6	705	154	-10	-1
Grasslands	21844	275	365	130	-91	-33	373	164	-98	-36	349	135	-75	-27
Croplands	12417	488	535	124	-47	-10	583	209	-95	-20	486	118	+2	0
Croplands and natural vegetation mosaic	5782	687	696	157	-9	-1	702	175	-15	-2	663	158	+24	+3
Global[3]	-	443	469	-	-	-6	475	-	-	-7	462	-	-	-4

[1]including open and closed shrublands. [2]including woody savannas and savannas. [3]for overlapped pixels with 1.5°×1.5° resolution.

Hydrol. Earth Syst. Sci. Discuss., https://doi.org/10.5194/hess-2018-638
Manuscript under review for journal Hydrol. Earth Syst. Sci.
Discussion started: 21 January 2019

Table 4- Comparison of interception estimated by Gerrits' model to STEAM and GLEAM through Average, RMSE, MBE and RE per land cover type. Negative MBE and RE show the Gerrits' model underestimates evaporation and vice versa. Average, RMSE and MBE are in mm $year^{-1}$ and RE is in %.

Land cover	Area	Gerrits	STEAM				GLEAM			
	$1000km^2$	Avg.	Avg.	RMSE	MBE	RE	Avg.	RMSE	MBE	RE
Evergreen needleleaf forest	5563	145	204	70	-58	-40	127	58	+18	+12
Evergreen broadleaf forest	11778	452	499	120	-47	-10	340	130	+111	+25
Deciduous needleleaf forest	2498	104	156	56	-53	-51	29	76	+74	+72
Deciduous broadleaf forest	1106	179	299	145	-120	-67	80	117	+99	+55
Mixed forest	13470	172	220	59	-48	-28	127	66	+45	+26
Shrublands[1]	29542	69	116	63	-47	-68	64	64	+5	+7
Savannas[2]	18846	162	246	107	-84	-52	107	79	+55	+34
Grasslands	21844	76	146	83	-70	-93	97	58	-22	-29
Croplands	12417	116	174	89	-58	-50	97	55	+19	+16
Croplands and natural vegetation mosaic	5782	166	243	108	-77	-46	112	89	+54	+33
Global[3]	-	128	183	-	-	-44	109	-	-	+15

[1]including open and closed shrublands. [2]including woody savannas and savannas. [3]for overlapped pixels with 1.5°×1.5° resolution.

Hydrol. Earth Syst. Sci. Discuss., https://doi.org/10.5194/hess-2018-638
Manuscript under review for journal Hydrol. Earth Syst. Sci.
Discussion started: 21 January 2019

Table 5- Comparison of transpiration estimated by Gerrits' model to STEAM and GLEAM through Average, RMSE, MBE and RE per land cover type. Negative MBE and RE show the Gerrits' model underestimates evaporation and vice versa. Average, RMSE and MBE are in mm year^{-1} and RE is in %.

Land cover	Area	Gerrits	STEAM				GLEAM			
	1000km^2	Avg.	Avg.	RMSE	MBE	RE	Avg.	RMSE	MBE	RE
Evergreen needleleaf forest	5563	284	222	122	+63	+22	259	100	+25	+9
Evergreen broadleaf forest	11778	915	619	347	+296	+32	890	163	+25	+3
Deciduous needleleaf forest	2498	234	177	82	+57	+24	261	71	-21	-12
Deciduous broadleaf forest	1106	617	538	192	+79	+13	570	120	+47	+16
Mixed forest	13470	390	305	147	+85	+22	363	114	+27	+7
Shrublands[1]	29542	133	137	85	+4	+3	159	81	-26	-20
Savannas[2]	18846	533	473	162	+59	+11	577	148	-44	-8
Grasslands	21844	199	214	109	+15	+7	233	93	-34	-17
Croplands	12417	372	393	131	-20	-5	371	90	+1	0
Croplands and natural vegetation mosaic	5782	521	444	159	+77	+15	530	112	-10	-2
Global[3]	-	315	276	-	-	+12	329	-	-	-4

[1]including open and closed shrublands. [2]including woody savannas and savannas. [3]for overlapped pixels with 1.5°×1.5° resolution.

Table 6- Comparison of mean annual evaporation estimated by Gerrits' model to Schreiber, Ol'dekop, Pike and Budyko through Average, RMSE, MBE and RE per land cover type. Negative MBE and RE show the Gerrits' model underestimates evaporation and vice versa. Average, RMSE and MBE are in mm $year^{-1}$ and RE is in %.

Land cover	area	Gerrits	Schreiber				Ol'dekop				Pike				Budyko			
	$1000km^2$	Avg.	Avg.	RMSE	MBE	RE	Avg.	RMSE	MBE	RE	Avg.	RMSE	MBE	RE	Avg.	RMSE	MBE	RE
Evergreen needleleaf forest	5563	430	348	136	+82	+19	415	110	+14	+3	387	117	+43	+10	380	119	+50	+12
Evergreen broadleaf forest	11778	1367	876	526	+491	+36	1065	355	+301	+22	991	419	+375	+27	966	443	+401	+29
Deciduous needleleaf forest	2498	338	250	110	+87	+26	291	85	+47	+14	273	94	+64	+19	270	96	+68	+20
Deciduous broadleaf forest	1106	796	636	22	+161	+20	727	120	+69	+9	687	152	+109	+14	680	160	+117	+15
Mixed forest	13470	563	420	185	+142	+25	506	134	+56	+10	470	150	+92	+16	461	156	+101	+18
Shrublands[1]	29542	203	250	84	-48	-24	273	99	-71	-35	263	91	-60	-30	261	90	-59	-29
Savannas[2]	18846	695	648	168	+47	+7	757	167	-62	-9	710	155	-15	-2	700	155	-5	-1
Grasslands	21844	275	346	134	-71	-26	372	152	-98	-36	359	141	-85	-31	358	140	-84	-31
Croplands	12417	488	502	154	-14	-3	566	181	-78	-16	538	164	-50	-10	533	162	-45	-9
Croplands and natural vegetation mosaic	5782	687	617	221	+69	+10	721	195	-35	-5	677	196	-10	-1	667	200	-20	-3
Global[3]	-	443	410	-	-	+8	471	-	-	-6	445	-	-	0	439	-	-	+1

[1]including open and closed shrublands. [2]including woody savannas and savannas. [3]for overlapped pixels with 1.5°×1.5° resolution.

Hydrology and Earth System Sciences
Open Access
Discussions

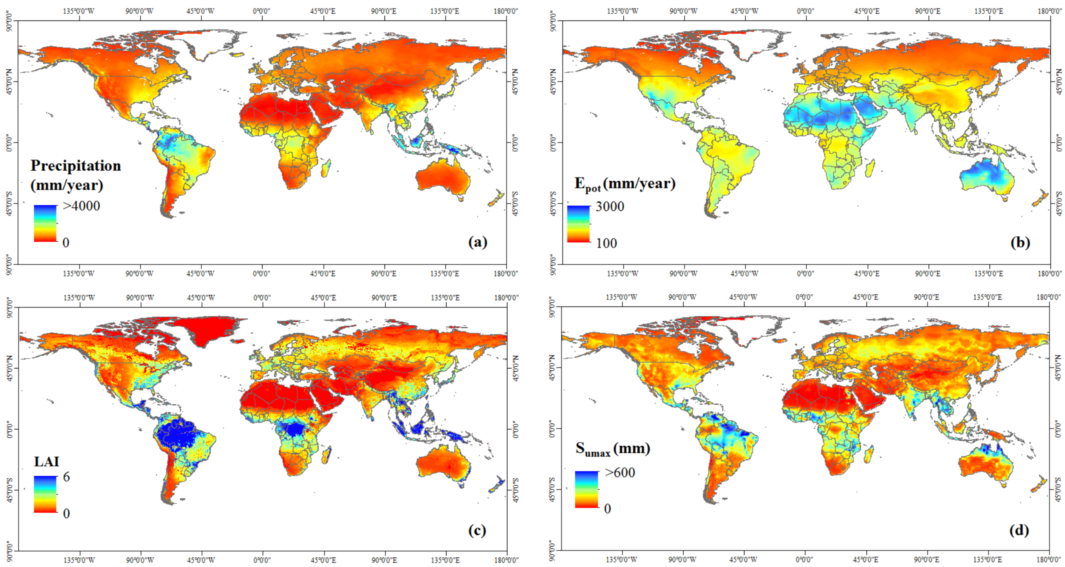

Figure 1- Mean annual of the applied data in the current study: (a) Precipitation (Ruane et al., 2015), (b) Potential evaporation (University of East Anglia Climatic Research Unit, 2014), (c) LAI (Zhu et al., 2013) and (d) $S_{u,max}$ (Wang-erlandsson et al., 2016).

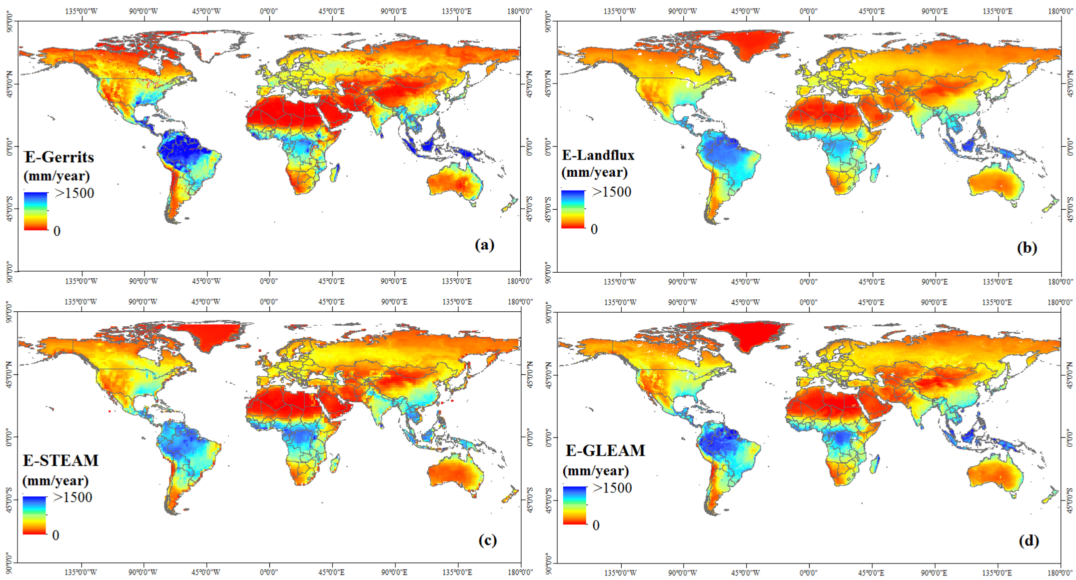

Figure 2- Mean annual evaporation estimated by (a) Gerrits' model, (b) Landflux-EVAL, (c) STEAM and (d) GLEAM.

Hydrol. Earth Syst. Sci. Discuss., https://doi.org/10.5194/hess-2018-638
Manuscript under review for journal Hydrol. Earth Syst. Sci.
Discussion started: 21 January 2019

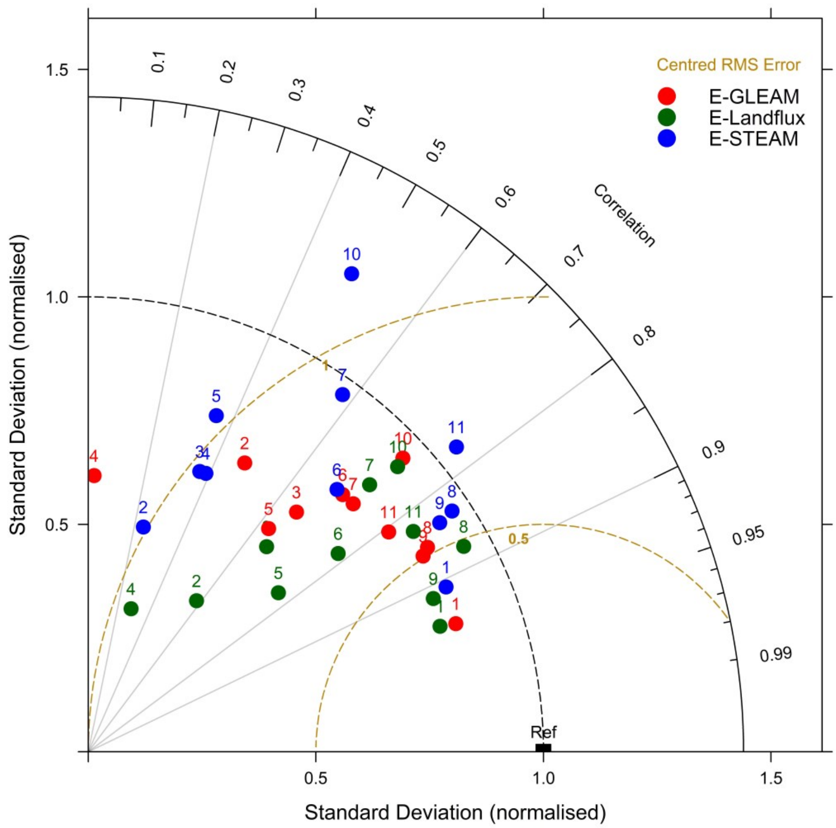

Figure 3- Taylor diagram for mean annual evaporation estimated by Gerrits' model in comparison to Landflux-EVAL (green circles), STEAM (blue circles) and GLEAM (red circles) for all data (No. 1), Evergreen Needleleaf Forest (No.2), Evergreen broadleaf forest (No. 3), Deciduous needleleaf forest (No. 4), Deciduous broadleaf forest (No. 5), Mixed Forest (No. 6), Shrublands (No. 7), Savannas (No. 8), Grasslands (No. 9), Croplands (No. 10) and Croplands and natural vegetation mosaic (No. 11).

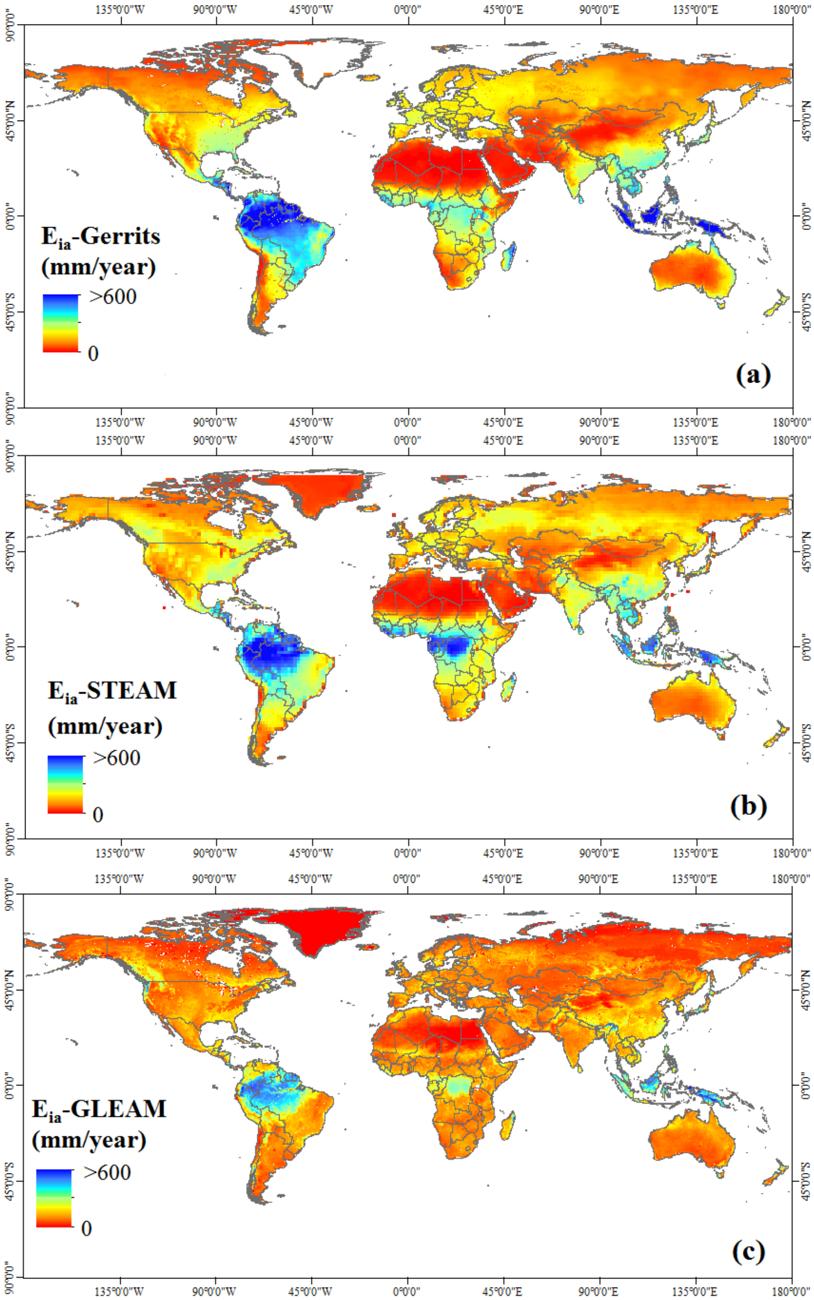

Figure 4- Simulated mean annual interception by (a) Gerrits' model and (b) STEAM and (c) GLEAM.

Hydrol. Earth Syst. Sci. Discuss., https://doi.org/10.5194/hess-2018-638
Manuscript under review for journal Hydrol. Earth Syst. Sci.
Discussion started: 21 January 2019

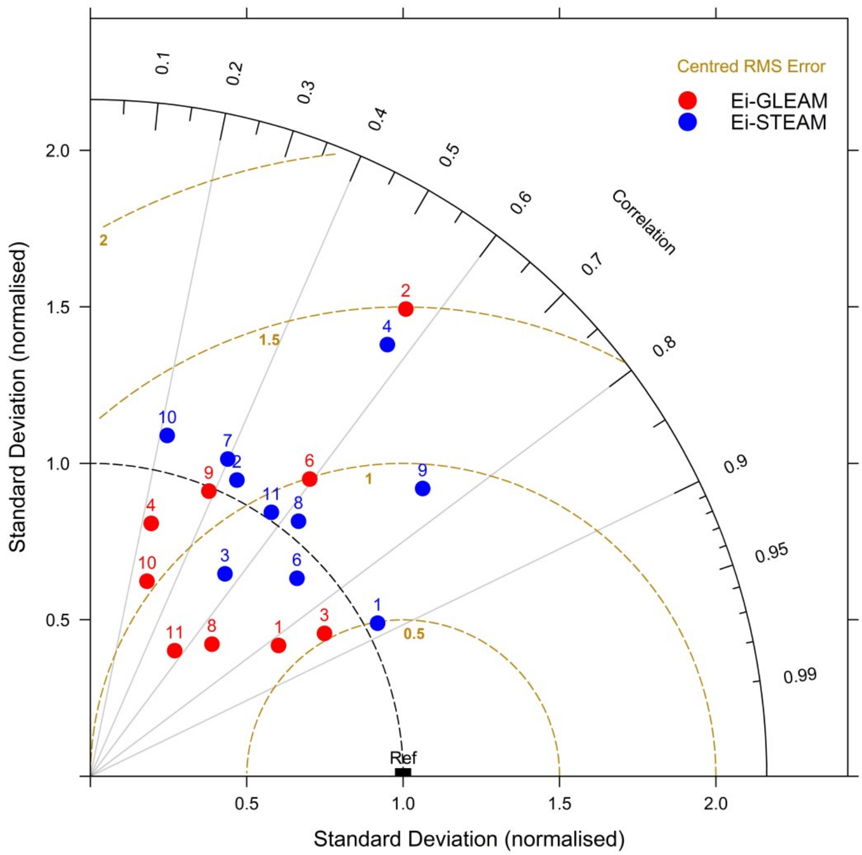

Figure 5- Taylor diagram for mean annual interception estimated by Gerrits' model in comparison to STEAM (blue circles) and GLEAM (red circles) for all data (No. 1), Evergreen Needleleaf Forest (No.2), Evergreen broadleaf forest (No. 3), Deciduous needleleaf forest (No. 4), Deciduous broadleaf forest (No. 5), Mixed Forest (No. 6), Shrublands (No. 7), Savannas (No. 8), Grasslands (No. 9), Croplands (No. 10) and Croplands and natural vegetation mosaic (No. 11).

Hydrol. Earth Syst. Sci. Discuss., https://doi.org/10.5194/hess-2018-638
Manuscript under review for journal Hydrol. Earth Syst. Sci.
Discussion started: 21 January 2019

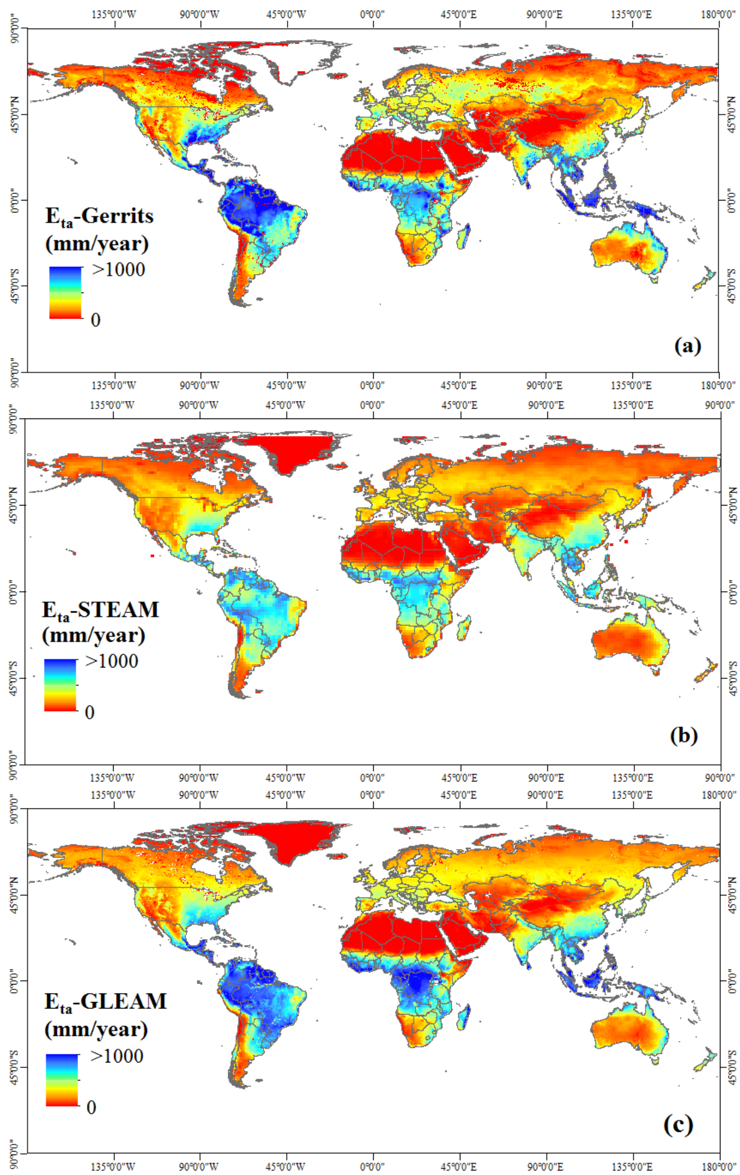

Figure 6- Simulated mean annual transpiration by (a) Gerrits' model, (b) STEAM and (c) GLEAM.

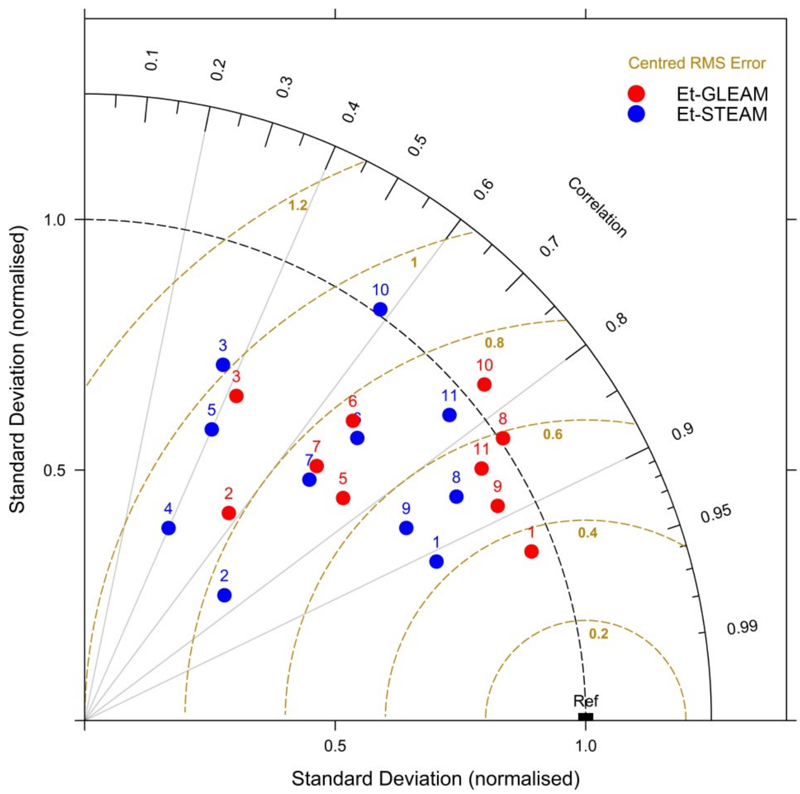

Figure 7- Taylor diagram for mean annual transpiration estimated by Gerrits' model in comparison to STEAM (blue circles) and GLEAM (red circles) for all data (No. 1), Evergreen Needleleaf Forest (No.2), Evergreen broadleaf forest (No. 3), Deciduous needleleaf forest (No. 4), Deciduous broadleaf forest (No. 5), Mixed Forest (No. 6), Shrublands (No. 7), Savannas (No. 8), Grasslands (No. 9), Croplands (No. 10) and Croplands and natural vegetation mosaic (No. 11).

Hydrol. Earth Syst. Sci. Discuss., https://doi.org/10.5194/hess-2018-638
Manuscript under review for journal Hydrol. Earth Syst. Sci.
Discussion started: 21 January 2019

Hydrology and Earth System Sciences
Open Access
Discussions

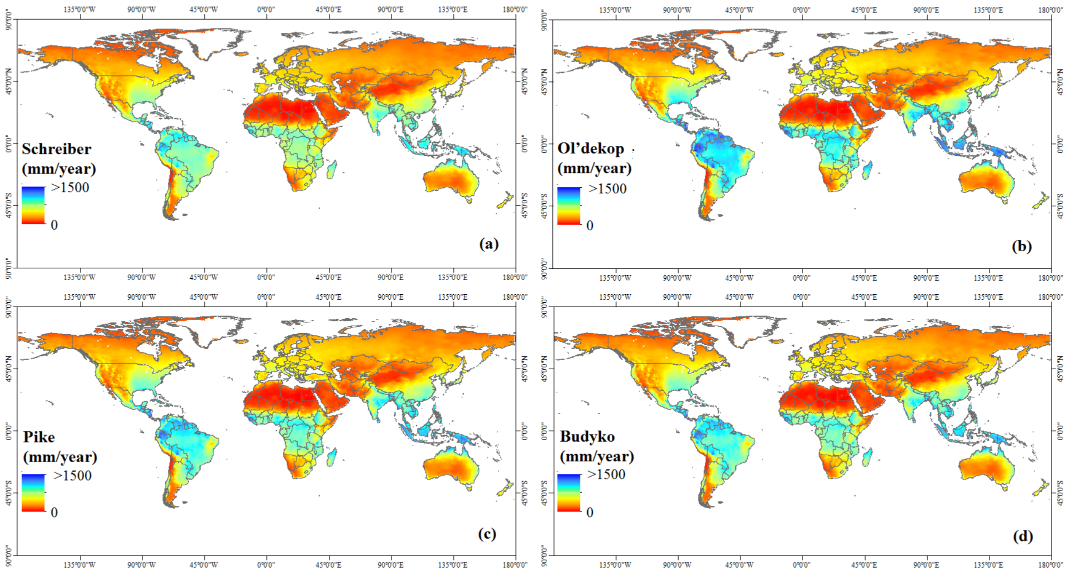

Figure 8- Global evaporation (mm year^{-1}) estimated by Budyko curves: (a) Schreiber (1904), (b) Ol'dekop (1911), (c) Pike (1964), and (d) Budyko (1974).

Hydrol. Earth Syst. Sci. Discuss., https://doi.org/10.5194/hess-2018-638
Manuscript under review for journal Hydrol. Earth Syst. Sci.
Discussion started: 21 January 2019

Hydrology and Earth System Sciences
Open Access
Discussions

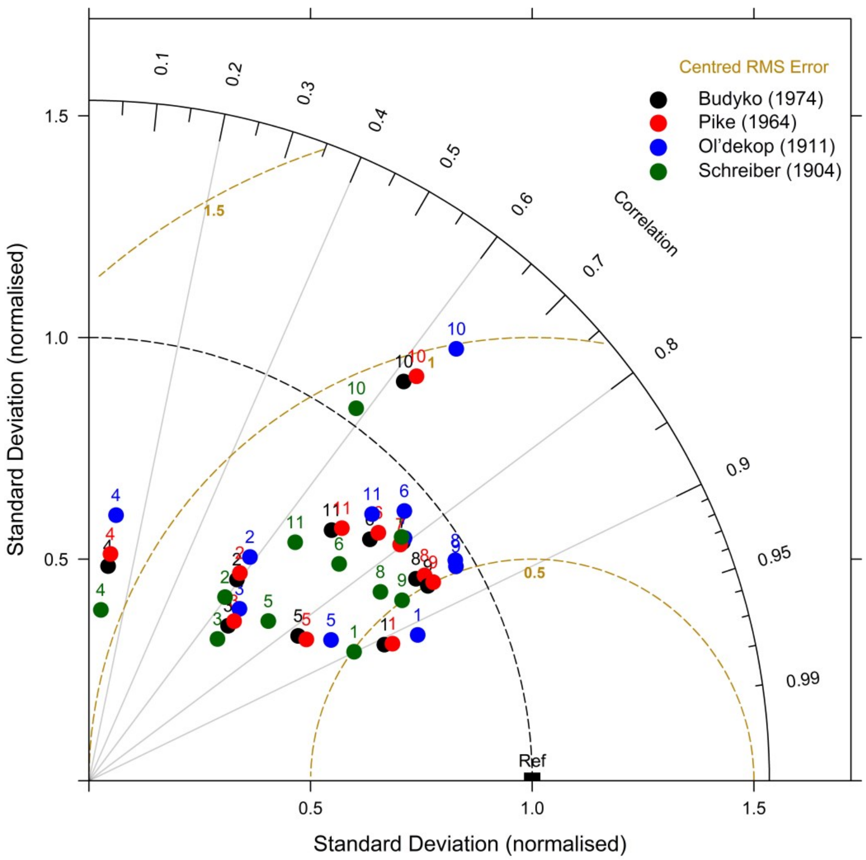

Figure 9- Taylor diagram for mean annual evaporation estimated by Gerrits' model in comparison to Schreiber (1904) (green circles), Ol'dekop (1911) (blue circles), Pike (1964) (red circles), and Budyko (1974) (black circles) for all data (No. 1), Evergreen Needleleaf Forest (No.2), Evergreen broadleaf forest (No. 3), Deciduous needleleaf forest (No. 4), Deciduous broadleaf forest (No. 5), Mixed Forest (No. 6), Shrublands (No. 7), Savannas (No. 8), Grasslands (No. 9), Croplands (No. 10) and Croplands and natural vegetation mosaic (No. 11).

Hydrol. Earth Syst. Sci. Discuss., https://doi.org/10.5194/hess-2018-638
Manuscript under review for journal Hydrol. Earth Syst. Sci.
Discussion started: 21 January 2019

Hydrology and Earth System Sciences
Open Access
Discussions

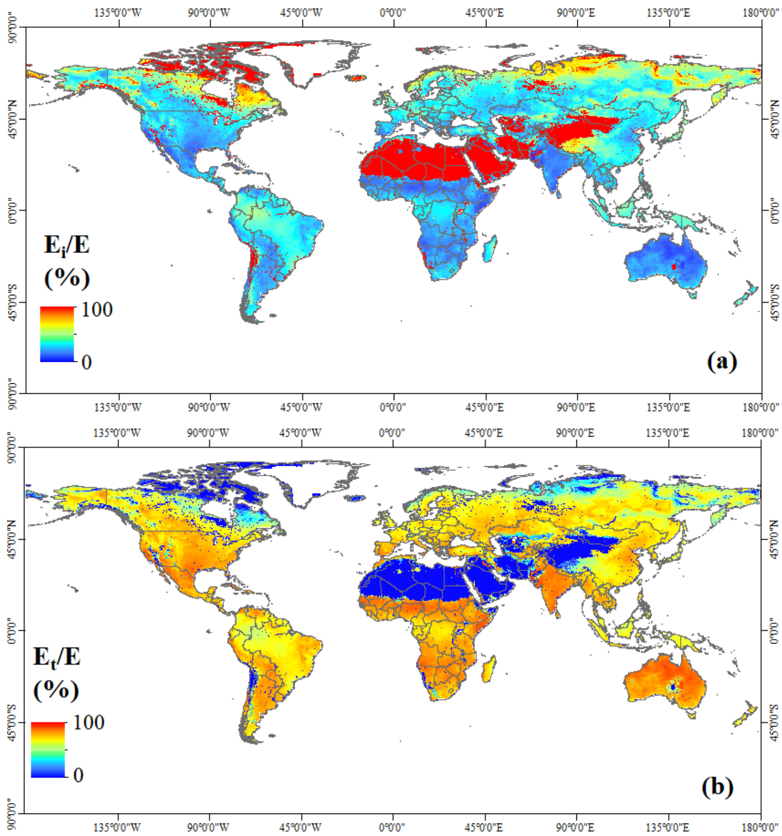

Figure 10- (a) Interception and (b) Transpiration ratio as a percentage of mean annual evaporation.